POLITECNICO DI TORINO
Repository ISTITUZIONALE

Monte Carlo approach to model the progressive failure of water distribution networks: application to a virtual city

(Article begins on next page)

04 August 2020

MONTE CARLO APPROACH TO MODEL THE PROGRESSIVE FAILURE OF WATER DISTRIBUTION NETWORKS: APPLICATION TO A VIRTUAL CITY

Veronica TAURINO[1], Omar KAMMOUH[1], Marco DOMANESCHI[1], Gian Paolo CIMELLARO[1]

ABSTRACT

The effects of the rapid urbanization and new hazards related to climate change are becoming extremely complex and unpredictable. Communities are thus seeking to improve their recovery capacity after catastrophic events through management and adaptation strategies. Generally, existing infrastructures have been built before the preparation of the seismic design guidelines, yielding to possible insufficient responses when subjected to earthquakes. Furthermore, interdependencies between different critical infrastructures is also becoming of paramount importance for improving community resilience. This paper focuses on the water distribution network as one of the most essential lifelines. The water distribution network is modeled using a specific software integrated by a mathematical toolbox. An earthquake scenario is applied to the water network and the related damages are determined by using fragility functions. The failure of the system occurs when the water flow and the water pressure go below a certain threshold. The resilience of the network is then evaluated using two indices: (i) the number of users without water and (ii) the drop in the total water supply.

Keywords: Resilience; Water Distribution Network; EPANET; Emergency Response; Earthquake; Virtual city.

1. INTRODUCTION

In the past, designers' efforts focused on the robustness and durability of lifeline systems. Today interest is shifting toward the concept of resilience, defined as the ability of the physical and non-physical infrastructure of a community to return to an ordinary level within a reasonable time following a disaster (Ellingwood et al, 2016, Cimellaro et al., 2010). The capability of infrastructures to restore its ordinary conditions after a certain hazardous event is the new focus. Bruneau, Chang et al. 2003 introduced the first definition of the community resilience, identifying its main features. Several authors presented different approach to quantify resilience (Kammouh et al. 2017; Franchin and Cavalieri, 2014). Some work focused mostly on the assessment of the restoration time of infrastructure (Kammouh and Cimellaro, 2017). Nevertheless, more work is still needed to define intrinsic countermeasures for communities to improve their resilience response against events like earthquakes.

In this study, the water distribution network (WDN) of a virtual city is considered. It is called IDEAL CITY and it consists in a tool to assess the reliability of infrastructures and their interdependency. The WDN is modeled using the software tool EPANET 2.0. After defining the network, earthquake scenarios are applied to study the effect of the seismic event on the network's components. The failure mechanism of the network has been simulated through a targeted removal of its components (e.g. pipelines) until a pre-defined failure state of the network is reached. Usually, the failure state is represented by going below a certain percentage of the water demand and the pressure at critical nodes.

The removal of the components is linked to the intensity of the seismic event, using fragility analyses. A Monte Carlo approach is adopted to generate failure configurations of the pipelines. Each pipeline is mapped to its corresponding removal probability derived from the fragility analysis to illustrate the targeted removal strategy. Then, the failure configurations have been used to assess the performance of the analyzed network. For each scenario, two resilience indices have been evaluated. The first one is

---

based on the number of people suffering the outage of water supply (Cimellaro et al., 2014) and the second considers the drop in the total water available.

Due to the large size of the network, many computational problems have been faced. To overcome such problems, several coding algorithms have been developed and presented in the paper.

2. RESILIENCE OF WATER NETWORK DISTRIBUTION

Currently, a standard procedure to evaluate the resilience of water networks is missing in the literature. A high serviceability of a water distribution network implies a high water supply with acceptable water pressure. Generally, the water supply depends on both the customer request and on the water pressure in the pipes. The earthquake induced damages result in a reduction of the water pressure and consequently in the water supply.

In this paper, a 24-hour demand pattern is defined according to the customer request in the virtual city. Two serviceability functions $F_1(t)$ and $F_2(t)$ are presented. The first is related to the number of people without water while the second measures the ratio between water supply and water demand. The mathematical equation of the first performance measure is:

$$F_1(t) = 1 - \frac{\sum_i n_e^i(t)}{n_{TOT}} \quad \text{for } i = 1, \dots N \tag{1}$$

where $n_e^i(t)$ is the number of people connected to node i suffering insufficient pressure; n_{tot} is the total number of people within the water distribution network; i is the generic node, N is the total number of nodes. The number of people without water at given node following a disaster event is assumed proportional to the water supply reduction at the same node:

$$n_e^i(t) = n_i \frac{w_{Lost}^i(t)}{w_i(t)} \tag{2}$$

where n_i is the total number of people connected to the node i; w_{Lost}^i is the volume of water lost at node i; w_i is the water demand at node i under normal operating conditions. The water loss and water demand at a given time step following a disaster event are computed as follows:

$$w_{Lost}^i(t) = \int_0^t \left[Q_{demand}(t) - Q_i(t) \right] dt \text{ for } i = 1, \dots N \tag{3}$$

$$w_i(t) = \int_0^t Q_{demand}(t) dt \tag{4}$$

Q_{demand} is the water demand at node i, Q_i is the available water flow (water supply) at node i, t is a generic time step. The second performance function $F_2(t)$ is related to the water demand and is given by the following formula:

$$F_2(t) = \frac{\sum_i Q_i(t)}{Q_{Demand,TOT}} \tag{5}$$

where $Q_{demand,tot}$ is the total water demand in the city. The recovery time T_R is assumed to last 24 hours (Figure 1). The Control Time T_c is considered equal to T_R in attempt to get a normalized value of resilience. In this specific case, resilience index for each scenario is equal to the average value of the serviceability.
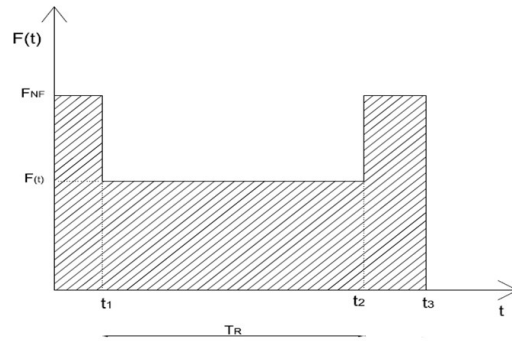
Figure 1. Functionality of Water Distribution Network (adapted from Cimellaro et al, 2015).

For each serviceability function, a resilience index is computed as the area below the function for the defined control time (Cimellaro et al, 2015):

$$R = \int_{t_1}^{t_2} \frac{F(t)}{T_c} dt \qquad (6)$$

3. IDEAL CITY: VIRTUAL CITY FOR RESILIENCE ANALYSES

Virtual city applications allow performing resilience analyses as information and data on the infrastructure are readily available. Currently, IDEAL CITY (Figure 2) is under development. It is a virtual city containing 890000 residents. The area is about 120 km^2 divided into 10 districts inspired by the real subdivision of the city of Turin in Italy. The inhabitants have been assigned to the districts in a way to create different population densities. Data and information about the city infrastructure are provided as separate layers in a GIS environment using "ArcGIS" software (ESRI, *ArcGIS)*.

Figure 2. IDEAL CITY: 3D representation ArcGIS" software (ESRI, *ArcGIS)*.

Currently, the layers include (Figure 3):
- Land use layer: structures and their occupancy class (residential, commercial, educational, administrative, military, etc.) besides the information respecting each land use, such as number of people, number of floors, and their surface area;
- Road layer: roads and streets;
- Pipe segment layer: material, flow quantity, diameter, slope according to the graphical coordinates, and junctions' information.
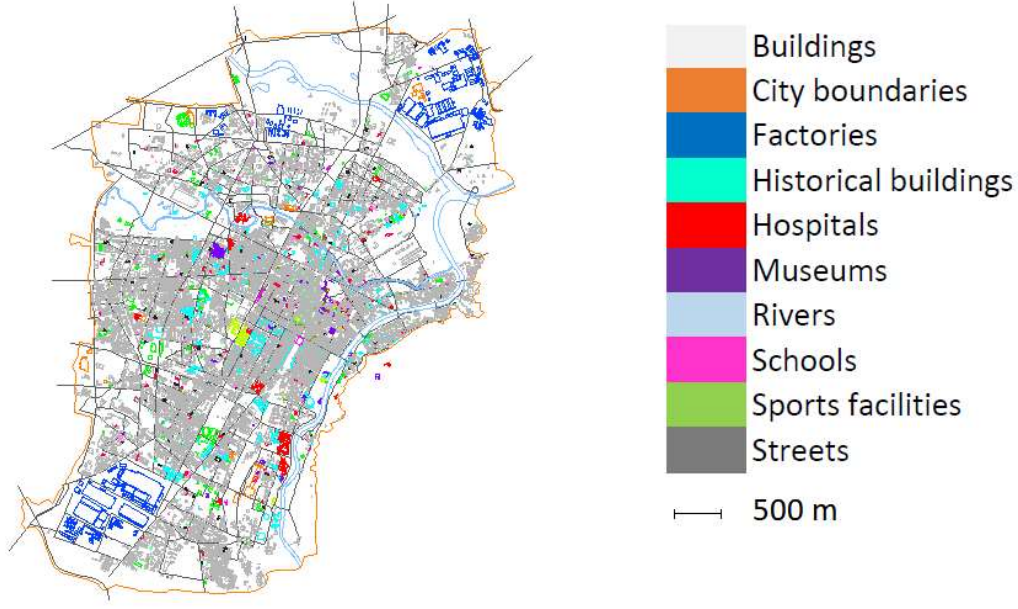
Figure 3. IDEAL CITY: buildings and road map.

4. MODEL DESCRIPTION, ASSUMPTION AND CALIBRATION

The water network analyzed in this study is based on the urban one of the city of Turin. Elevations of the grounds have been obtained from Google Maps (Google, *Google Maps Elevation API*).

Several assumptions had to be made for preparing the water network model. The geometry of the water network is assumed to overlap the transportation network, as it was not possible to have more details about due to security reasons. The water network model (Figure 4) has been built using the EPANET-Matlab toolkit (Eliades, 2017; United States Environmental Protection Agency *EPANET,* 2008; MathWorks *MATLAB*).

The EPANET model comprises 19654 ductile iron pipes (1,285,007 m of total length) with a Darcy-Weisbach roughness coefficient εequal to 0.26 mm, 14996 nodes, 9 valves, 38 pumps, 19 reservoirs, and 26 tanks. Nodes are situated 1.2 m below the ground surface. Ground elevations range between 207.76m and 340.68 m above sea level. Water sources are aquifer (82%) and other sources such as rivers and surface water (18%) with an average total daily demand of 353.38Ml/day.

The water demand at each node (junction) depends on the number of people who are served by that node. Therefore, it is first necessary to find the population density per each unit volume of household, which also depends on the district as the population density is not the same among all districts. This is done using the following formula:

$$\rho_j = \frac{P_{e_j}}{V_j} \left[\frac{people}{m^3} \right] \tag{7}$$

where ρ_j is the household population density in district j (number of people per a unit volume of a household located in district j), Pe_j is the number of people in district j, V_j is the total volume of the households located in district j.

Figure 4. Global view of the water network: 19604 pipes.

The water network in the IDEAL CITY model consists in a mesh of interconnected pipes. Each mesh element (closed shaped) is associated to a demand with respect to the total volume of household located inside:

$$q_{w,j} = \rho_j \cdot \delta \cdot V_w \qquad (8)$$

where $q_{w,j}$ is the water demand of the mesh element w in district j, δ is the city water supply per inhabitant (equal to 315 l/capita/day) (Piemonte R.), V_w is the volume of the households within mesh element w. The total water demand per mesh element $q_{j,w}$ is distributed equally among the adjoining nodes (Figure 5a). In other words, the water demand for each node is the sum of the demand contribution of the adjoining mesh elements (Figure 5b):

$$q_i = \sum_{w=1}^{n_{w,i}} \frac{q_{w,j}}{n_{w,i}} \qquad (9)$$

where q_i is the water demand at node i, $q_{w,j}$ if the water demand of the mesh element w which is located in district j, $n_{w,i}$ is the number of mesh elements adjoining node i, $n_{i,w}$ is the number of the nodes adjoining mesh w.
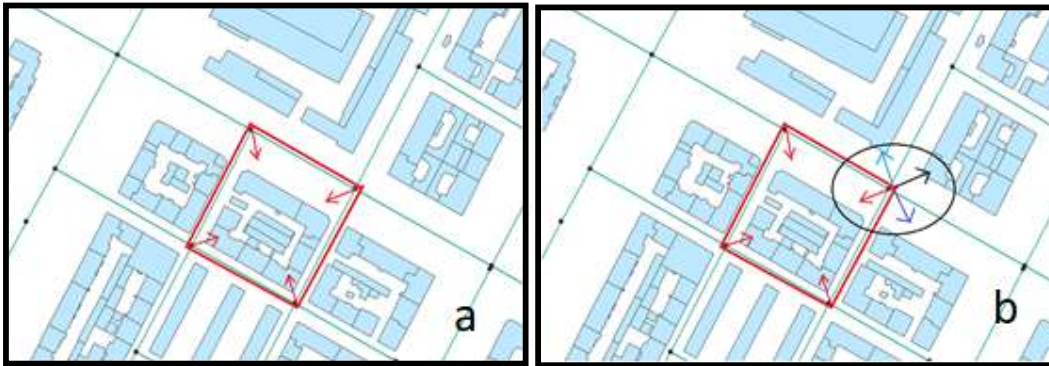

Figure 5. (a) Water demand $q_{j,w}$ for the mesh element w, (b) water demand for the i-node.

The calibration of a WDN of such a size brings on several difficulties. It is a fundamental issue to ensure

5

an accurate and realistic simulation for both the flow velocity and the pressure. The pipes diameters, the positions of the valves, pumps, reservoirs and tanks, have been determined with the following constraints (Figure 6):

$$0.5m/s \leq \text{velocity} \leq 2m/s \tag{10}$$

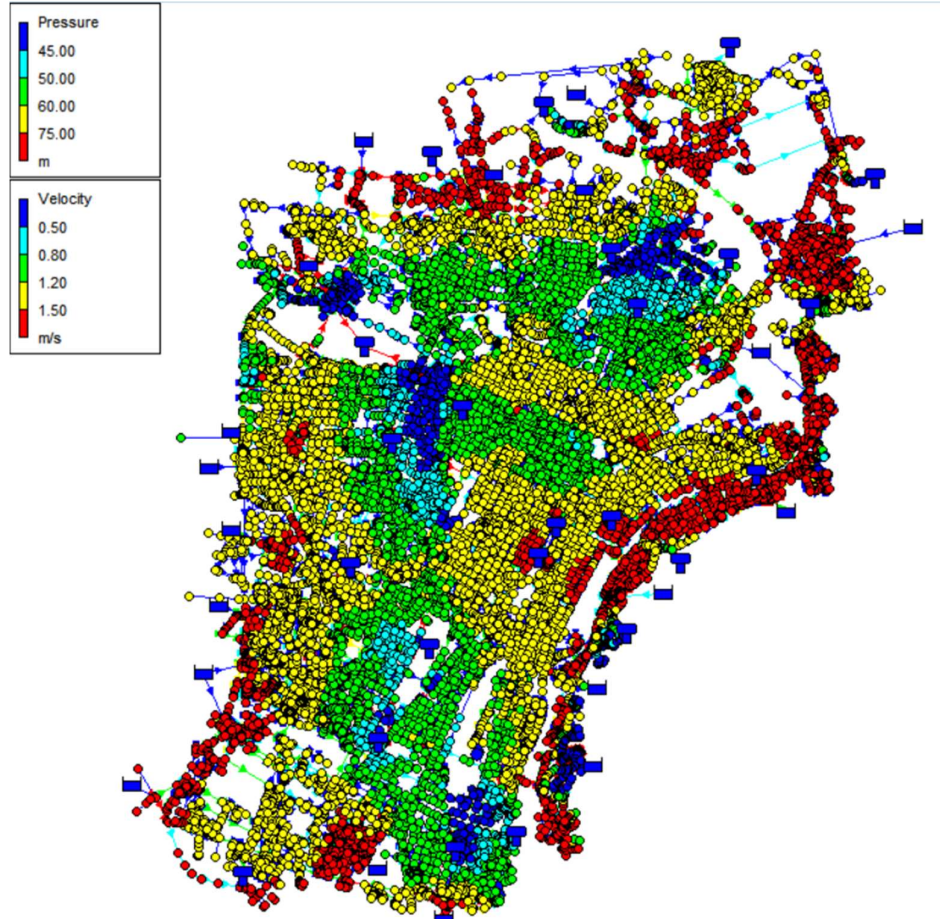$$40m \leq \text{pressure} \leq 80m \tag{11}$$

Figure 6. Calibrated WDN - velocity constraint refers to the pipes, pressure constraints to the nodes.

The calibration procedure adopted in this paper is iterative. Future work will be oriented to apply a systematic parametric calibration for large-scale water networks (Lingireddy and Ormsbee, 1997; Afshar and Kazemi, 2012; Parehkar et al, 2015).

5. SEISMIC HAZARD AND EARTHQUAKE DAMAGE OF PIPES

The seismic hazard is evaluated through a probabilistic approach (PSHA, Probabilistic Seismic Hazard Analysis) according to the Italian code (Baker, 2013). The hazard is expressed as the occurrence probability of a seismic event of specific features within a certain period of time. The corresponding ground motion (peak ground acceleration PGA) has a P probability of exceedance in T years, return period.
The Italian National Institute of Geophysics and Volcanology (INGV) provides disaggregation hazard maps for the whole Italian territory. These maps allow identifying the contributions of different seismic sources to the hazards of a site. The most common form of disaggregation is the two-dimensional magnitude M and distance R: it allows identifying the contributions of seismic sources at a distant R

from a specific site and capable to generate an earthquake of magnitude *M* (Figure 7). The disaggregation process therefore provides the predominant earthquake on the scenario hazard, that is the event with magnitude *M* at distance *R* from the site that contributes most to the seismic hazard of the site itself. Therefore, given a constant soil condition, the intensity of the ground shaking at the site depends on *M* and *R* values, even though the empirical ground motion deviates from the median value predicted. The INGV database can be queried for different probability of exceedance in a chosen time interval (usually 50 years) or a specified return period.
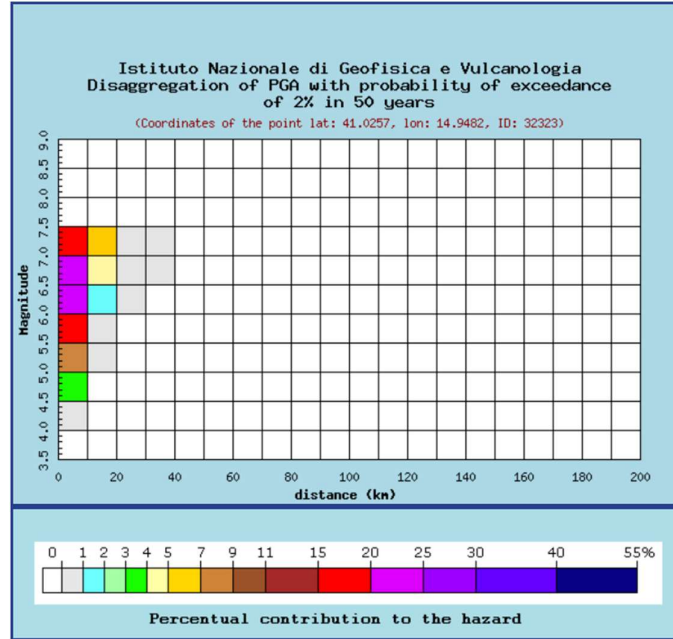

Figure 7. Disaggregation hazard map for 2% PE in 50 years (Return Period = 2475 years).

In this work, the return period assessed is 2475 years with a probability of exceedance of 2% in 50 years. According the attenuation law by Sabetta and Pugliese 1996, the *PGV* value is influenced by the soil local condition and it is a function of *M* and *R*:

$$Log\, PGV = a + bM + cLog\sqrt{R^2 + h^2} + e_1 S_1 + e_2 S_2 \pm \sigma \tag{12}$$

where a, b, e_1, e_2, are parameters determinate through multiple non-linear regression, h is a function of the depth, σ is the standard deviation of logarithm of PGV, S_1 and S_2 depends on geological soil conditions, M and R are respectively the magnitude and the epicenter distance of the scenario earthquake resulting from the seismic hazard evaluation.
In our case study, the PGV value is 35.84cm/s and it is assumed as constant across the entire region of interest.

6. FRAGILITY ANALYSIS OF WATER PIPES

The reliability of a water pipe network is connected with the concept of fragility of its elements. Herein, focus is given to the pipes as the most important components of the pipe network because it is the most challenging part for inspection and replace.
The seismic fragility of the buried pipelines as discussed in the American Lifelines Alliance (ALA, 2001) (Eidinger, 2001) is adopted in this work. Fragility functions are entirely empirical and are based on reported damage from historical earthquakes. Damage is expressed in terms of pipe repair rate *RR*, defined as the number of repairs per 1,000 m of pipe length exposed to a particular level of seismic demand.

$$RR = 0.00187 \cdot K_1 \cdot PGV \tag{13}$$

where K_1 is a coefficient that depends on the pipe material, pipe diameter, joint type, and soil condition. Once the repair rate is known, the failure probability $P_{f,j}$ of a pipeline is evaluated through the Poisson exponential probability distribution, as follows:

$$P_{f,j} = 1 - e^{-RR \cdot L} \tag{14}$$

where L is the length of pipe and $e^{-RR \cdot L}$ is the probability of zero breaks along the pipe. In this paper three different K_1 are considered in order to investigate the influence of pipe material on the failure probability $P_{f,j}$: $K_1 = \{0.5; 0.8; 1\}$.

The seismic wave propagation induces strains to the pipes due to the soil-pipe interaction: strains could produce damage if the pipe strength is exceeded. When pipe damage occurs, the pipe is assumed to break in the middle.

A demand driven analysis DDA is carried out in standard procedure by the software EPANET. The DDA procedure fixes the demand at the nodes of the network. When a pipe damage occur, pressure drops at some nodes. The water supply is affected by the pressure drop, thus a pressure driven analysis PDA is carried out to take into account the dependence of water supply on pressure.

Pipe damage is modeled (C.U. School of Civil Environmental Engineering, 2008) with EPANET2.0 as follows: the pipe is divided into two equal parts and two reservoirs are added at their endpoints in order to simulate the water leakage through the crack (Figure 8). The reservoirs have a total head equal to the elevation of the middle point of the pipe (as the pipe breaks in the middle). A check valve is inserted so that water only flow towards the reservoirs.
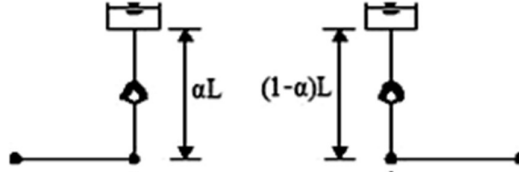

Figure 8. Pipe break simulation in EPANET 2.0 (C.U. School of Civil Environmental Engineering, 2008).

Under ideal operating conditions, the WDN pressures and velocities range between precise limits defined by the Italian prescriptions. In the case of pipe damage, the pressure at some nodes drops. To take into account scenarios in which the demand is fully dependent on the pressure, a PDA is carried out. First, damaged pipes are introduced in the model and a standard DDA runs. Then, nodes with pressure below value required to satisfy the demand, are converted in Emitter nodes (Rossmann, 2000). An Emitter is a node whose demand is proportional to a fractional power of the pressure according the follow equation:

$$Q_i = C_i (H_i - z_i)^{\alpha} = C_i \cdot p_i^{\alpha} \tag{15}$$

where Q_i is the actual demand flow; C_i is the emitter coefficient; H_i is the actual total head of the i_{th} node; z_i is the elevation of the i_{th} node; p_i is the actual pressure of the node; and α is the emitter exponent (0.5 if no other information are available). Emitter coefficient is evaluated as:

$$C_i = \frac{Q_{demand}}{(H_{r,i} - z_i)^{\alpha}} = \frac{Q_{demand}}{p_{r,i}^{\alpha}} \tag{16}$$

where Q_{demand} is the demand flow; $H_{r,i}$ and $p_{r,i}$ are respectively the total head and the pressure required to satisfy Q_{demand}. Herein 20 m of water column is assessed the minimum value to satisfy the demand at the nodes. The software runs again with emitters inserted.

The PDA procedure is applied during the breakage. Three cases can occur:
- $Q_i \leq 0$, the actual demand flow at the node is equal to zero,
- $0 \leq Q_i \leq Q_{demand}$, the actual demand flow is equal to Q_i;
- $Q_i \geq Q_{demand}$, the actual demand flow is equal to Q_{demand}.

EPANET software does not allow any upper bound for the equation above mentioned, moreover negative flow values have no physical meaning: the *PDA* can be corrected in order to reach a more accurate solution.

7. DEFINITION OF THE EVENT SCENARIOS

Resilience is a dynamic quantity characterized by a lack of certainty. Uncertainties are crucial for both risk management and resilience analysis (Bozorgnia and Bertero, 2004). A Monte Carlo method has been used to generate a large number of simulations in order to study the uncertainty through a Matlab code (Fragiadakis, Vamvatsikos and Christodoulou, 2012). The code input consists in the pipe diameters, lengths, start and end nodes, with the pipe failure probability. In addition, an importance factor has been assigned to each pipeline: "2" is assigned to main pipelines, "1.5" to the pipes within the districts, and "1" to the connection pipes between the districts. The number of scenarios N_S herein considered is 5000, which yielded a stable distribution of the results (Figure 9).
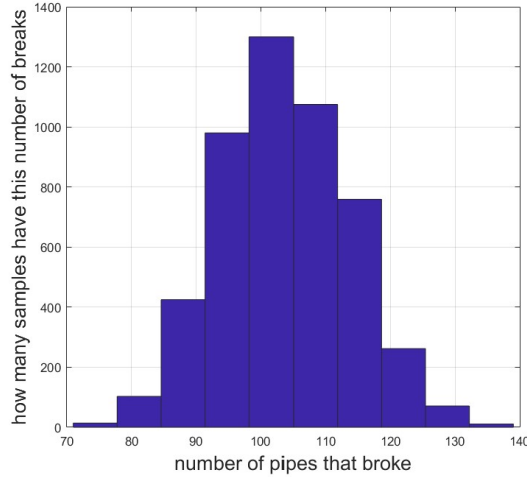

Figure 9. Distribution of scenarios events. The total number of scenarios is 5000. $K_1 = 0.5$.

8. NUMERICAL RESULTS

Serviceability functions $F_1(t)$ and $F_2(t)$ are evaluated for the 5000 simulation scenarios and for three values of K_1. An earthquake random occurrence is considered in the simulations. For each of them, the resilience index has been computed using equations (6). At each earthquake occurrence time, the mean value of the resilience indices has been computed with its standard deviation (Figure 10). Pipes with ductile material (low K_1) show a more resilient behavior than pipes with fragile material (high low K_1). The highest resilience indices correspond to $K_1 = 0.5$.

It is clear that the resilience indicators are not very sensitive to the arrival time of the earthquake. In addition, the value R follows the water demand pattern: it is lower when a damage occurs during a high water demand hour.

Moreover, the resilience index R_Q (referring to the variation of water supply) is more sensitive than the index R (referring to people suffering with water outage).
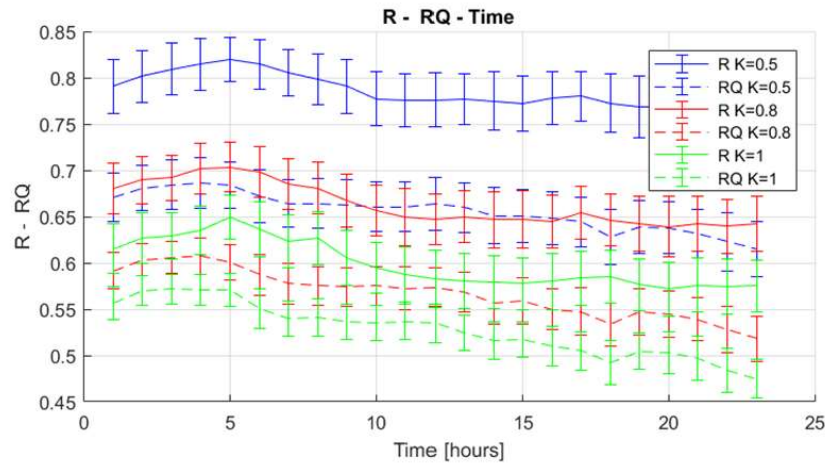
Figure 10. Resilience indices R and R_Q for three K_1 values (pipe material).

9. CONCLUDING REMARKS

Two resilience indices to measure the performance of a water distribution network after an earthquake are proposed. The methodology presented herein considers the pipes as the only element of the WDN that can be affected by an earthquake. The methodology has been applied to a virtual city, namely IDEAL CITY. Two serviceability function are identified. The first $F_1(t)$ is related to the number of users suffering water outage while the second $F_2(t)$ is related to the reduction in the total water supply. Finally, resilience indices are evaluated as the area under the performance curves. Both resilience indices show different values but they both follow the daily water demand trend.

The introduced methodology can be useful as a decision making tool for assessing the resilience of water distribution systems. Future works will aim at extending and generalizing the presented methodology. Since the water demand pattern, time control, and recovery time affect the evaluation of resilience, future work will also focus on a parametric study to understand the effect of each parameter on the resilience evaluation. The methodology will also include the possibility of modifying both the seismic input and the geometry of the network.

10. ACKNOWLEDGEMENTS

11. REFERENCES

Afshar A and Kazemi H (2012). Multi objective calibration of large scaled water quality model using a hybrid particle swarm optimization and neural network algorithm, *KSCE Journal of Civil Engineering*, 16(6): p. 913-918.

Baker JW (2013). An introduction to probabilistic seismic hazard analysis, *White Pap*, 2(1): p. 79.

Bozorgnia Y and Bertero VV (2004). Earthquake engineering: from engineering seismology to performance-based engineering, *CRC press*.

Bruneau M et al. (2003). A framework to quantitatively assess and enhance the seismic resilience of communities, *Earthquake spectra*, 19(4): p. 733-752.

Cimellaro G P, Reinhorn A M, and Bruneau M (2010). "Framework for analytical quantification of disaster resilience." *Engineering Structures*, 32(11), 3639–3649.

Cimellaro G P, Solari D, and Bruneau M (2014). "Physical infrastructure interdependency and regional resilience index after the 2011 Tohoku earthquake in Japan." *Earthquake Eng. Struct. Dyn.*, 43, 1763.

Cimellaro GP et al. (2015). New resilience index for urban water distribution networks, *Journal of Structural Engineering*,142(8): p. C4015014.

Cimellaro G P, Renschler C, Reinhorn AM, and Arendt L (2016). "PEOPLES: a framework for evaluating resilience." Journal of Structural Engineering, ASCE, 142(10), 1-13 DOI: 10.1061/(ASCE)ST.1943-1541X.0001514.

Cimellaro GP et al. (2016). Resilience of Critical Structures, Infrastructure, and Communities, *Pacific Earthquake Engineering Research Center (PEER)*, Berkeley, California, pp. 318.

C.U. School of Civil Environmental Engineering (2008). Giraffe User's Manual.

Eidinger J (2001). Seismic fragility formulations for water systems. Sponsored by the American Lifelines Alliance, G&E Engineering Systems Inc.

Eliades D, *OpenWaterAnalytics/EPANET-Matlab-Toolkit*. *https://it.mathworks.com/matlabcentral/fileexchange/25100-openwateranalytics-epanet-matlab-toolkit.*

Ellingwood BR et al. (2016). The Centerville Virtual Community: a fully integrated decision model of interacting physical and social infrastructure systems, *Sustainable and Resilient Infrastructure*, 1(3-4): p. 95-107.

ESRI. ArcGIS, *http://www.esri.com/arcgis/about-arcgis*.

Fragiadakis M, Vamvatsikos D and Christodoulou SE (2012). Reliability assessment of urban water networks, *15th world conference on earthquake engineering,* Lisbon, Portugal.

Franchin P, Cavalieri F (2014). Probabilistic assessment of civil infrastructure resilience to earthquakes. *Computer Aided Civil And Infrastructure Engineering*, 30(7), 583–600. DOI: 10.1111/mice.12092.

Google, *Google Maps Elevation API*. https://developers.google.com/maps/documentation/elevation/intro.

Kammouh O, Dervishaj G and Cimellaro GP (2017). A New Resilience Rating System for Countries and States. *Procedia Engineering* 198 (Supplement C): p. 985-998.

Kammouh O et al. (under review). Resilience Evaluation of Urban Communities Based on Peoples Framework. *ASCE-ASME Journal of Risk and Uncertainty in Engineering Systems, Part A: Civil Engineering*.

Kammouh O, Dervishaj G, and Cimellaro GP (2018). Quantitative Framework to Assess Resilience and Risk at the Country Level. *ASCE-ASME Journal of Risk and Uncertainty in Engineering Systems, Part A: Civil Engineering* 4(1): p. 04017033.

Kammouh O et al. (2017). Resilience Quantification of Communities Based on Peoples Framework. *16th World Conference on Earthquake Engineering (16WCEE)*. Santiago, Chile: IAEE.

Kammouh O and Cimellaro GP (2017). Restoration Time of Infrastructures Following Earthquakes. *12th International Conference on Structural Safety & Reliability*. Vienna, Austria: IASSAR.

Kammouh O, Cimellaro GP, and Mahin SA (under review). Downtime estimation and analysis of lifelines after earthquakes. *Journal of Engineering Structure*.

Lingireddy S, Ormsbee LE, and Wood DJ (1997). Calibration of Hydraulic Network Models, *Water Encyclopedia*.

MathWorks. MATLAB, *www.mathworks.com/products/matlab.htm*.

Parehkar A et al. (2015) Auto Calibration and Optimization of Large-Scale Water Resources Systems*, World Academy of Science, Engineering and Technology, International Journal of Environmental, Chemical, Ecological, Geological and Geophysical Engineering*, 8(3): p. 233-239.

Piemonte R, Indagini e studi finalizzati alla predispozione del Piano di Tutela delle Acque, *http://www.regione.piemonte.it,* Italy.

Protezione civile. Hazard maps, *http://www.protezionecivile.gov.it, http://esse1-gis.mi.ingv.it/,* Italy.

Rossmann LA (2000). EPANE2.0: user manual.

Sabetta F and Pugliese A (1996). Estimation of response spectra and simulation of nonstationary earthquake ground motions*, Bulletin of the Seismological Society of America*, 86(2): p. 337-352

United States Environmental Protection Agency (2008). EPANET, *https://www.epa.gov/water-research/epanet*, Ohio.